Fault tolerant control of an hexacopter with a tilted-rotor configuration

Juan I. Giribet
GPSIC - Facultad de Ingeniería
Universidad de Buenos Aires
Instituto Argentino de Matemática - CONICET
Buenos Aires, Argentina
Email: jgiribet@fi.uba.ar

Claudio D. Pose
GPSIC - Facultad de Ingeniería
Universidad de Buenos Aires
Buenos Aires, Argentina
Email: cldpose@fi.uba.ar

Ignacio Mas
Instituto Tecnológico de Buenos Aires
CONICET
Buenos Aires, Argentina
Email: imas@itba.edu.ar

***Abstract*—Recently, it was shown that an hexagon-shaped hexa-rotor micro aerial vehicle with unidirectionally spinning tilted rotors is capable of fault tolerant attitude and altitude control. This result has been theoretically proven and validated by simulations. However, experimental results have never been reported yet. In this work experimental results are presented, and a comparison between a tilted-rotor hexacopter with one in a standard rotor configuration is carried out.**

***Index Terms*—Fault tolerant control, Unmanned aerial vehicle, Actuator allocation.**

I. Introduction

Multi-rotor micro aerial vehicles (MAVs) have become very popular in recent years, due to the fact that the electronic systems needed to fly them have dramatically increased their availability and usefulness, decreasing their cost and weight. Simplicity and cost-effectiveness have turned out to be very appealing and, as a consequence, an increasing number of applications have risen in many fields, such as agriculture, surveillance, and photography, among others. Fault tolerance has been addressed in the literature as a matter of high importance, in particular for multi-rotor vehicles, see for instance [1], [2], [3], [4] and references therein.

Particularly, the minimum number of rotors needed to achieve a fault tolerant control has been discussed in [6], [7], [8], [9] among others. In [8], [9], the capability of compensating for a rotor failure without losing the ability to exert torques in all directions, and therefore keeping full attitude control in case of failure was studied. To this end, the method proposed in [8] to compensate for rotor failure makes use of a special kind of motor electronic speed controller (ESC), which allows for motor bidirectional operation. This method has several disadvantages. First, this kind of ESC is quite uncommon in practice. Second -and more importantly- changing the speed direction of the rotors generates thrust in the opposite direction if the propeller is not automatically adapted.

For this reason a simpler method was proposed in [9] that guaranteed fault tolerant full attitude control. The method consists of changing the orientation of the rotors.

A scheme of an hexagon-shaped hexacopter is shown in Figures 1 and 2, with its rotors tilted an angle γ. It is known that for the standard configuration ($\gamma = \pi/2$), it is not possible to achieve full attitude control in case of rotor failure ([5], [8], [9]). However, in [9] it was proved that there exists $\gamma \neq \pi/2$ such that the tilted-rotor configuration can achieve full attitude control under failure of one rotor.

A question that naturally arises at this point concerns the criterion for determining the γ angle. It is expected to have a trade-off in the selection of this angle, between the capability to reject torque disturbances and the ability to exert vertical thrust on the vehicle, this problem has been studied in [9], where an admissible loss of thrust is defined (5%) and the angle is chosen in such a way that maximizes the (worst case) torque disturbance that can be rejected if one rotor fails.

It must be pointed out that configurations with tilted rotors

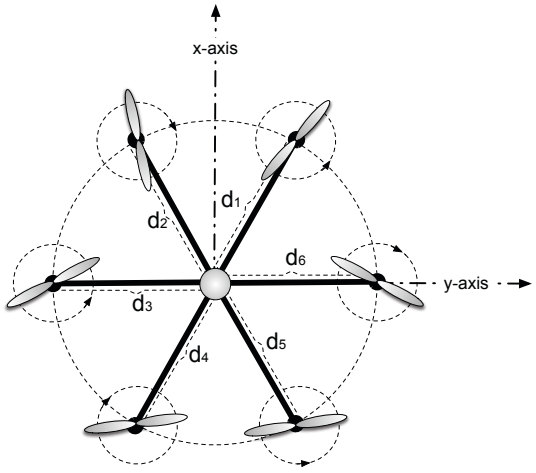

Figure 1. Hexacopter axes configuration (top view).

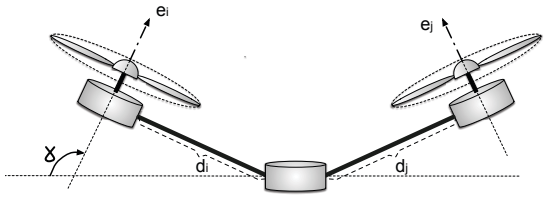

Figure 2. Hexacopter axes configuration (side view).

(or tilted arms) are presently found in commercial solutions. Presumably, this tilting is not present for fault tolerant control purposes but to improve vehicle stability. This configuration also renders a wider field of view when a camera is placed underneath the vehicle.

This article is organized as follows. Section 2 introduces the notation used in this work. Section 3 presents the vehicle model and how to study the failure of one rotor. Section 4 describes the testbed used to obtain the experimental results, which are shown in Section 5. Finally, Section 6 draws the conclusions.

II. Notation

Given a matrix $X \in \mathbb{R}^{n\times m}$, $N(X)$ denotes its kernel and $X^\dagger \in \mathbb{R}^{m\times n}$ its Moore-Penrose pseudo-inverse. $X \in \mathbb{R}^{n\times m}$, $\tilde{X}_i \in \mathbb{R}^{n\times m}$ denotes the matrix X, with the *i*-th column replaced by zeros. This matrix will be used when referring to a motor failure in the *i*-th motor. For a vector $x \in \mathbb{R}^n$, its *i*-th component is denoted by x_i.

A vector $x \in \mathbb{R}^n$ will be called non–negative (positive), and denoted $x \geq 0$ ($x > 0$) , if each of its components is a non–negative (positive) number, i.e., $x_1 \geq 0, \ldots, x_n \geq 0$ ($x_1 > 0, \ldots, x_n > 0$). The following notation will be used in the sequel: $c\gamma = \cos\gamma$ and $s\gamma = \sin\gamma$.

III. Vehicle model

Each motor exerts a force $f_i \in [0, F_M]$. In practice, each motor is commanded through a Pulse Width Modulated (PWM) signal u_i, which goes from 0 to 100%. Near the nominal operating point, a linear relation between the PWM signal and the exerted force is assumed, with $f_i = k_f u_i$. It is also considered that each motor exerts a torque on its spinning axis, $m_i = (-1)^i k_t u_i$. The k_f and k_t, constants are usually established experimentally. The constant $\tilde{k}_t := \frac{k_t}{k_f}$ is defined as it will be used in what follows, for the sake of clarity.

As it was mentioned above, by tilting the rotors an angle γ (as seen in Figure 2), fault tolerant control can be achieved without losing control neither in attitude nor in the vertical direction (thrust), even with a faulty motor. Here it is assumed that the hexarotor has the fault tolerant configuration of Figure 2.

The length of the arm, measured from the center of the vehicle to the motor axis along the arm, is denoted $l = \|d_i\|$, with $i = 1, ..., 6$. The angle γ will be the tilting angle of the motor, measured as depicted in Figure 2. To simplify the notation, a parameter α is defined in the following way:

$$\alpha = \alpha(\gamma) = \frac{\tilde{k}_t}{\sqrt{3}\ l \tan(\gamma)}. \tag{1}$$

In [9, Theorem 3], it was shown that if this parameter is chosen such that $0 < |\alpha| < 1$ then fault tolerance can be achieved. Furthermore, if $|\alpha| = 1$ or $\alpha = 0$ ($\gamma = \pi/2$) then the hexarotor is not completely controllable if one rotor fails. In what follows, it is assumed that $0 < |\alpha| < 1$.

Let M_x, M_y and M_z, be the control torques exerted by the motors on the vehicle. Also let F_z be the resultant force exerted by the motors along the vehicle's z axis. When all motors are working properly, the relation between the (M_x, M_y, M_z, F_z) 4-tuple, and the f forces vector is given by the following equation:

$$\begin{bmatrix} M_x \\ M_y \\ M_z \\ F_z \end{bmatrix} = A(\gamma,\alpha)\cdot f, \qquad \text{with} \qquad f = \begin{bmatrix} f_1 \\ \vdots \\ f_6 \end{bmatrix}. \tag{2}$$

The force-torque matrix $A = A(\gamma,\alpha) \in \mathbb{R}^{4\times 6}$ is given by,

$$A = \tag{3}$$
$$\begin{bmatrix} \tilde{k}_t c\gamma[& -1 & \frac{\alpha+1}{2\alpha} & \frac{\alpha+1}{2\alpha} & -1 & \frac{\alpha-1}{2\alpha} & \frac{\alpha-1}{2\alpha}] \\ \tilde{k}_t\sqrt{3}c\gamma[& -\frac{1}{3\alpha} & \frac{3\alpha-1}{6\alpha} & -\frac{3\alpha-1}{6\alpha} & \frac{1}{3\alpha} & \frac{3\alpha+1}{6\alpha} & -\frac{3\alpha+1}{6\alpha}] \\ \tilde{k}_t s\gamma[& 1 & -1 & 1 & -1 & 1 & -1] \\ -s\gamma[& 1 & 1 & 1 & 1 & 1 & 1] \end{bmatrix}.$$

In order to mathematically represent the case of a failure in the *i*-th rotor, the A force-torque matrix, should be replaced by matrix $\tilde{A}_i$, then:

$$\begin{bmatrix} M_x \\ M_y \\ M_z \\ F_z \end{bmatrix} = \tilde{A}_i(\gamma,\alpha)\cdot f \tag{4}$$

The problem to study consists in solving the following inverse problem: given a desired torque-force 4-tuple (M_x, M_y, M_z, F_z), it is desired to find $f \in \mathbb{R}^6$ that solves equation (4). As stated before, in order to be valid, a solution must be positive, since the force that the motors can exert is only in one direction. Furthermore, the forces' modulus, must be lower than the maximum thrust that motors can generate, i.e., $f_i \in [0, F_M]$, for $i = 1, ..., 6$. It has sense to concentrate on the positivity of $f \in \mathbb{R}^6$, since this is the reason why the standard hexacopter is not fault tolerant.

The most common and frequently used solution for equation (4) relies on the Moore-Penrose pseudo-inverse of $\tilde{A}_i(\gamma,\alpha)$, as it gives the minimum norm solution and consequently minimize the energy needed. However, as it was shown in [10], the Moore-Penrose pseudo-inverse not always is the best alternative, since it sometimes gives solutions that don't satisfy the forces constraints.

Given a desired torque–force $(M_x, M_y, M_z, F_z) \in \mathbb{R}^4$ with thrust $F_z > 0$, the set of solutions of equation (4) can be written as:

$$f = \underbrace{\tilde{A}_i^\dagger(\gamma,\alpha)\cdot \begin{bmatrix} M_x \\ M_y \\ M_z \\ F_z \end{bmatrix}}_{f_0} + \beta w, \tag{5}$$

with $w \in N(\tilde{A}_i)$, $\beta \in \mathbb{R}$ and f_0 being the minimal euclidean norm given by the Moore-Penrose pseudinverse.

$$\tilde{A}_1^\dagger = \begin{bmatrix} 0 & 0 & 0 & 0 \\ \frac{\alpha\left(6\alpha^3+9\alpha^2+1\right)\sec(\gamma)}{2k_t\left(3\alpha^2+1\right)^2} & \frac{\alpha\left(9\alpha^3+9\alpha-2\right)\sec(\gamma)}{2\sqrt{3}k_t\left(3\alpha^2+1\right)^2} & -\frac{(3\alpha+1)^2\csc(\gamma)}{12\left(3k_t\alpha^2+k_t\right)} & \frac{(\alpha-1)^2\csc(\gamma)}{12\alpha^2+4} \\ \frac{\alpha\sec(\gamma)}{6k_t\alpha^2+2k_t} & -\frac{\sqrt{3}\alpha^2\sec(\gamma)}{6k_t\alpha^2+2k_t} & \frac{\csc(\gamma)}{4k_t} & \frac{\csc(\gamma)}{4} \\ -\frac{6\alpha^4\sec(\gamma)}{k_t\left(3\alpha^2+1\right)^2} & \frac{2\alpha\sec(\gamma)}{\sqrt{3}k_t\left(3\alpha^2+1\right)^2} & -\frac{\csc(\gamma)}{9k_t\alpha^2+3k_t} & \frac{\alpha^2\csc(\gamma)}{3\alpha^2+1} \\ -\frac{\alpha\sec(\gamma)}{6k_t\alpha^2+2k_t} & \frac{\sqrt{3}\alpha^2\sec(\gamma)}{6k_t\alpha^2+2k_t} & \frac{\csc(\gamma)}{4k_t} & \frac{\csc(\gamma)}{4} \\ \frac{\alpha\left(6\alpha^3-9\alpha^2-1\right)\sec(\gamma)}{2k_t\left(3\alpha^2+1\right)^2} & -\frac{\alpha\left(9\alpha^3+9\alpha+2\right)\sec(\gamma)}{2\sqrt{3}k_t\left(3\alpha^2+1\right)^2} & -\frac{(1-3\alpha)^2\csc(\gamma)}{6k_t\left(6\alpha^2+2\right)} & \frac{(\alpha+1)^2\csc(\gamma)}{12\alpha^2+4} \end{bmatrix} \quad (6)$$

$$\tilde{A}_2^\dagger = \begin{bmatrix} -\frac{\alpha\left(15\alpha^3+9\alpha^2+9\alpha-1\right)\sec(\gamma)}{4k_t\left(3\alpha^2+1\right)^2} & -\frac{\alpha\left(9\alpha^3+27\alpha^2-9\alpha+5\right)\sec(\gamma)}{4\sqrt{3}k_t\left(3\alpha^2+1\right)^2} & \frac{(3\alpha+1)^2\csc(\gamma)}{12\left(3k_t\alpha^2+k_t\right)} & \frac{(\alpha-1)^2\csc(\gamma)}{12\alpha^2+4} \\ 0 & 0 & 0 & 0 \\ \frac{3\alpha(\alpha+1)^3\sec(\gamma)}{4k_t\left(3\alpha^2+1\right)^2} & -\frac{\alpha(3\alpha-1)^3\sec(\gamma)}{4\sqrt{3}k_t\left(3\alpha^2+1\right)^2} & \frac{(1-3\alpha)^2\csc(\gamma)}{6k_t\left(6\alpha^2+2\right)} & \frac{(\alpha+1)^2\csc(\gamma)}{12\alpha^2+4} \\ -\frac{\alpha(3\alpha-1)\sec(\gamma)}{4\left(3k_t\alpha^2+k_t\right)} & \frac{\sqrt{3}\alpha(\alpha+1)\sec(\gamma)}{4\left(3k_t\alpha^2+k_t\right)} & -\frac{\csc(\gamma)}{4k_t} & \frac{\csc(\gamma)}{4} \\ \frac{\alpha\left(3\alpha^3-1\right)\sec(\gamma)}{k_t\left(3\alpha^2+1\right)^2} & \frac{\alpha\left(9\alpha^3+1\right)\sec(\gamma)}{\sqrt{3}k_t\left(3\alpha^2+1\right)^2} & \frac{\csc(\gamma)}{9k_t\alpha^2+3k_t} & \frac{\alpha^2\csc(\gamma)}{3\alpha^2+1} \\ \frac{\alpha(3\alpha-1)\sec(\gamma)}{4\left(3k_t\alpha^2+k_t\right)} & -\frac{\sqrt{3}\alpha(\alpha+1)\sec(\gamma)}{4\left(3k_t\alpha^2+k_t\right)} & -\frac{\csc(\gamma)}{4k_t} & \frac{\csc(\gamma)}{4} \end{bmatrix}$$

A. *Fault tolerant control*

In this work, fault tolerance is understood as the capability of the vehicle to achieve torque in any direction even if one rotor is failing.

Without loss of generality, due to vehicle symmetry, only the case of a failure in motor number 2 will be considered. The behavior of motors 4 and 6 can be explained by applying a rotation in the z-axis. For failures in rotors 1, 3, and 5, besides the rotation, a reflection is needed because one motor rotates clockwise while the other rotates counter-clockwise. The Moore-Penrose pseudoinverses for $\tilde{A}_1 = \tilde{A}_1(\gamma, \alpha)$ and $\tilde{A}_2 = \tilde{A}_2(\gamma, \alpha)$ are given in equation (6).

For a failure in motor 2, observe that matrix $\tilde{A}_2^\dagger$ can be decomposed as a block matrix $\tilde{A}_2^\dagger = \begin{bmatrix} P & Q \end{bmatrix}$, with $P \in \mathbb{R}^{6\times 3}$ and $Q \in \mathbb{R}^6$. Also, notice that if $\alpha = 0$ or $|\alpha| = 1$ then for some $i = 1, ..., 6$, the component $Q_i = 0$. In fact, if $\alpha = 0, \alpha = 1$ or $\alpha = -1$ then $Q_5 = 0, Q_1 = 0$ or $Q_3 = 0$, respectively. Also, notice that the kernel of $\tilde{A}_2$ is given by,

$$N(\tilde{A}_2) = span\left\{ \overbrace{\begin{pmatrix} \frac{3}{4}\ (\alpha-1)(\alpha+\frac{1}{3}) \\ 0 \\ -\frac{3}{4}(\alpha+1)(\alpha-\frac{1}{3}) \\ -\frac{3}{4}(\alpha^2+\frac{1}{3}) \\ \alpha \\ \frac{3}{4}(\alpha^2+\frac{1}{3}) \end{pmatrix}}^{w}, \begin{pmatrix} 0 \\ 1 \\ 0 \\ 0 \\ 0 \\ 0 \end{pmatrix} \right\}.$$

Of course, it only has sense to consider $w \in N(\tilde{A}_2)$, because motor 2 is assumed to be not working.

To show why a vehicle with $\alpha = 0$ (i.e., $\gamma = \pi/2$) or $|\alpha| = 1$ is not fault tolerant, suppose that $Q_i = 0$ (either because $\alpha = 0$ or $|\alpha| = 1$), and observe that then $w_i = 0$. Now, let $P_i \in \mathbb{R}^3$ be the i-th row of matrix $P \in \mathbb{R}^{6\times 3}$, and consider a torque $[M_x\, M_y\, M_z]^T = -P_i$. Then, according to equation (5), $f_i = -\|P_i\|^2 < 0$ for every $F_z \geq 0$. Hence it is not possible to find $f \geq 0$ that achieves the torque $-P_i$. On the other hand, if $0 < |\alpha| < 1$, observe that $N_i > 0$, for every $i = 1, ..., 6$ then with a thrust $F_z > 0$ high enough, it is always possible to find $f \geq 0$ that achieves a given torque.

IV. Experimental setup

In order to obtain experimental results and compare the non-tilted and tilted hexarotor, two vehicles were built, as shown in Figures 3 and 4.

The frame is the DJI-F550, with a maximum distance between motors of 550mm. The actuators installed on this frame are T-Motor 2212-920KV motors, with 9545 plastic self-tightening propellers, driven by 20A electronic speed controllers (ESC). As this frame only allows to mount the motors pointing upwards, a mechanical adapter was 3D printed to achieve the tilted motor configuration, while the distance from the motor to the center of mass remains the same. The battery used is a 3S 5000mAh 20C LiPo that allows approximately 15 minutes of hovering flight (without failures).

Figure 3. Vehicles used for experiments. Left: tilted-motor hexacopter . Right: standard hexacopter.

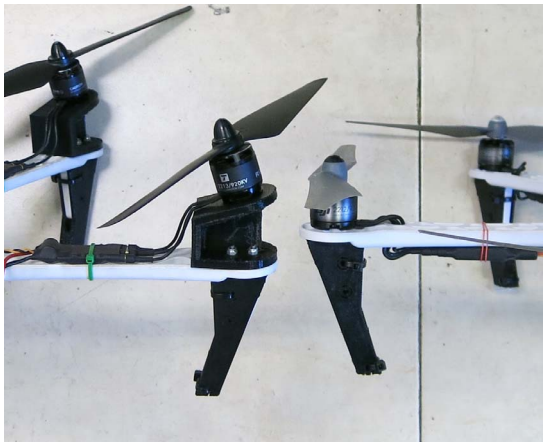

Figure 4. Detail of rotor mounting configuration. Left: tilted-motor hexacopter . Right: standard hexacopter.

The flight computer used is a custom-designed board [11] developed by the GPSIC Lab to support experiments that are usually carried out on this kind of vehicles. It is based on the LPC-1769 microcontroller, an ARM Cortex M3 that runs at 120MHz, and several sensors such as the MPU-6000 IMU, the HMC5883L digital compass and the BMP180 barometer, sending flight information to MATLAB (for data analysis) through a 57600bps XBee wireless connection. The control loop runs at 200Hz, where the pitch, roll, and yaw angles are estimated and a PID control algorithm calculates the torque for vehicle stabilization. Then, the allocation algorithm gives the force of each motor in order to achieve the desired torque, and a simple function converts this value into the PWM signals commanded to the ESC.

The only difference in the control algorithm between the non-tilted and tilted vehicles is the allocation step, because it takes into account the rotor disposition on each case in order to achieve the corresponding torque. All the parameters for the experiments are shown in Table I, as well as the PID controller constants K_d, K_p and K_i (derivative, proportional and integral terms, respectively):

Table I
VEHICLE TECHNICAL SPECS AND PID CONSTANTS

Variable	Value	Units
l (arm length)	0.26	m
P (weight)	2.1	kg
F_M (max. thrust)	0.644	kg
γ	107	deg
k_f	0.0776	N/%
k_t	0.0077	N/%
$\tilde{k}_t$	0.1	-
$K_d(PID)$	0.5	Nm/(rad/s)
$K_p(PID)$	1.4	Nm/rad
$K_i(PID)$	0.1	Nm/rad.s

V. EXPERIMENTAL RESULTS

To validate the proposed approach, experimental results are conducted with both the non-tilted and tilted hexacopters in similar flight situations, where a fault is intentionally introduced.

Given the characteristics of the vehicles used, the fault applied is partial, i.e., a motor is limited to 40% of its maximum thrust. A partial failure is not uncommon for multirotor vehicles, see for instance [4]. In our case, the reason behind this selection is to generate enough total thrust (lift) during the fault situation to maintain the vehicle in the air, as the focus of this work is to achieve torque in any direction. A vehicle with different mass and thrust capabilities would handle a total motor failure without losing lift under the same principles.

Therefore, given a known partial failure affecting one of the motors, the experiments consist of showing the differences in controllability for the tilted and non-tilted vehicles. As the detection and/or identification of the failure is out of the scope of this work, it is considered perfectly known. Using an on-off switch on the remote controller of the vehicle, a non-failure or failure situation can be selected, while simultaneously - and instantaneously– changing the allocation algorithm that considers the failure.

In the first experiment, both vehicles attempt to take off in both a nominal situation and while presenting a failure. The results are shown in Figures 5 and 6, respectively. First, a take-off without failure is performed, to demonstrate that the vehicles indeed hover in a very similar way.

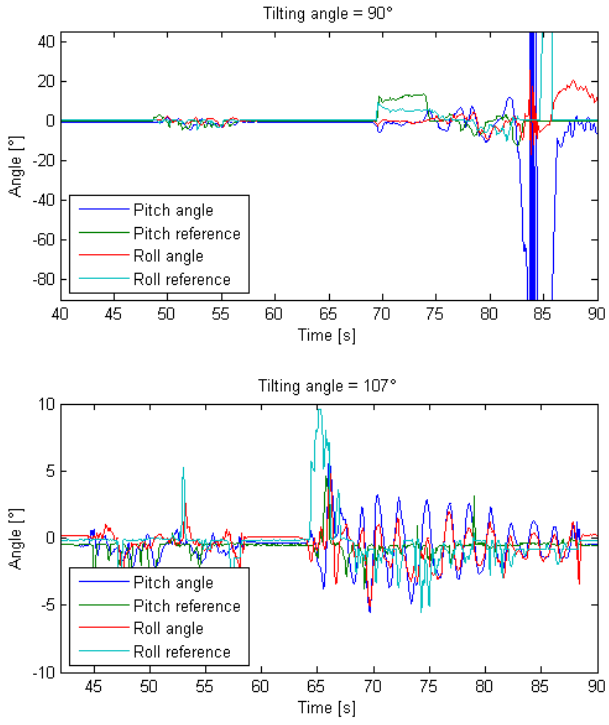

Figure 5. Angles of the vehicles during take-off with failure

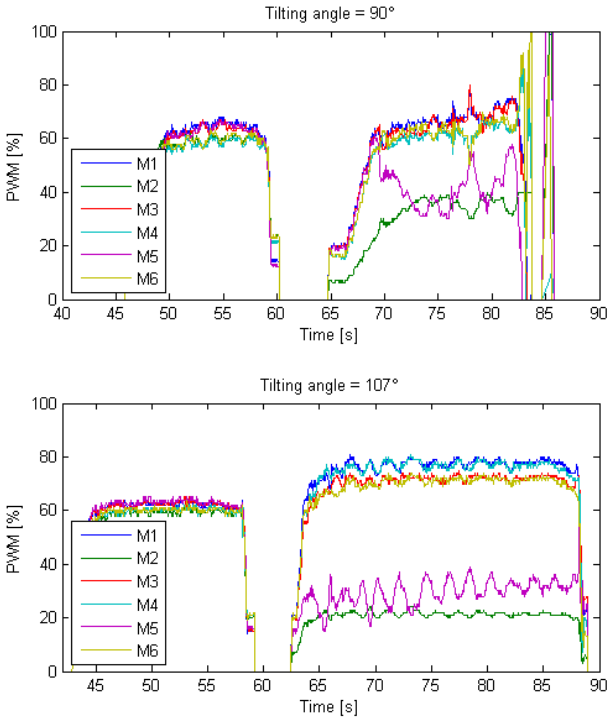

Figure 6. PWM signals of the vehicles during take-off with failure

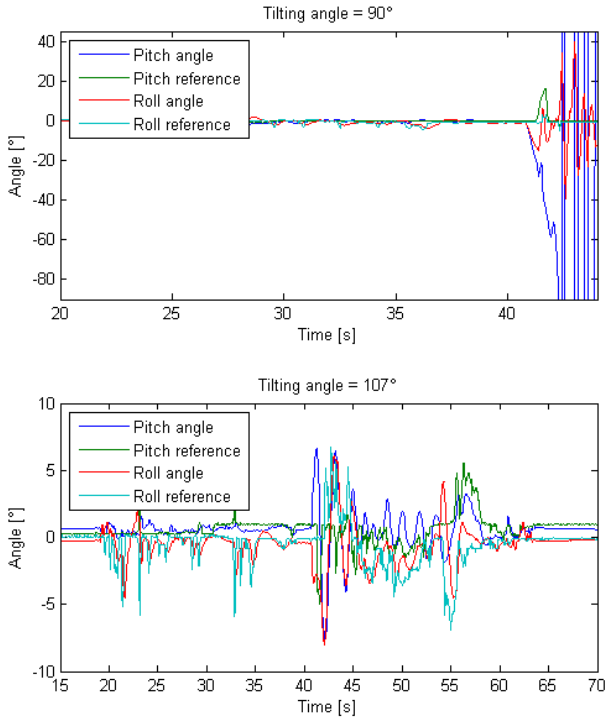

Figure 7. Angles of the vehicles during in-flight failure

Figure 5 shows that the roll and pitch angles during the non-failure take-off remain within a 3 degree range (45 to 60 seconds) for both vehicles. Then the vehicles land and a new take-off is attempted with the failure in motor 2 at 65 seconds. The upper graphic shows the non-tilted vehicle which –after several seconds trying to make a stabilized take-off– finally does a half barrel roll and crash lands. The lower graphic presents the roll and pitch angles for the tilted vehicle, which executes a successful take-off, lightly oscillating at the beginning due to ground effect, and then maintaining the attitude within a 3 degree range, similarly to the non-failure case. Finally, it lands at 88 seconds.

In Figure 6, the PWM signals for the motors of both vehicles are shown for the same time period depicted in the previous figure. During the non-failure flight, the PWM signals are similar, around 60%, for both vehicles. When the failure is imposed, the PWM signal of motor 2 in the non-tilted vehicle, reaches its maximum 40% and saturates during take-off, causing the crash. Meanwhile, the tilted vehicle's PWM signals are within range and achieve a successful flight.

The second experiment consists of activating the failure while the vehicle is flying, and observing if the vehicle can recover the hovering state. This experiment is carried out because, as the ground effect causes disturbances, it may be considered as the reason which prevents the non-tilted vehicle from taking off in the previous experiment. The results for this experiment are shown in Figures 7 and 8.

The upper plots in both figures show the non-tilted vehicle's

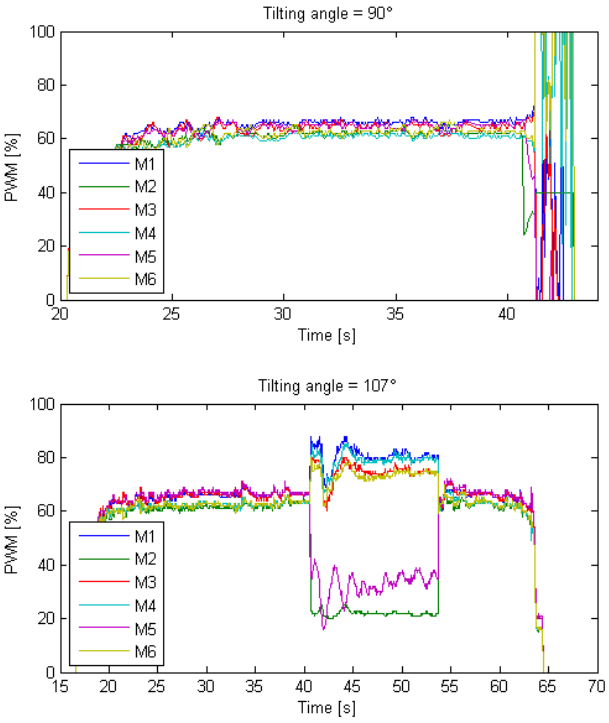

Figure 8. PWM signals of the vehicles during in-flight failure

angles and PWM, respectively, which show that the vehicle is well stabilized until the failure is activated. When the failure is applied, motor 2 saturates almost instantly and produces a crash in a new half barrel roll. The lower plots, also in both figures, show the failure activating for the tilted-motor at 40 seconds, and the vehicle oscillating during a short period of time and stabilizing again. Finally, at 54 seconds the failure is disabled, and then the vehicle lands safely.

A key difference between the two vehicles is that, when the non-tilted vehicle achieves a brief hovering state (as seen at around t=41s in Figure 8, upper plot), the PWM signal for motor 2 is around 35%, which explains why, when faced with a minimal disturbance, the motor saturates almost immediately. On the other hand, the hovering-state PWM signal for motor 2 in the tilted vehicle with a fault is around 22% (Figure 8, lower plot), which gives the motor a larger signal range to reject disturbances, as it is far away from the 40% signal saturation limit.

It should be noted that, for the tilted vehicle, flight performance during failure is not as good as when the failure is not present. This is expected as the system is degraded while the control law remains the same.

VI. Conclusion

This article presented experimental results showing fault tolerance of an hexagon-shaped hexa-rotor with a titled-rotor configuration. The behavior of the fault-tolerant vehicle is compared to that of one in a standard rotor configuration in similar flight situations. The results validate the theoretical developments indicating that fault tolerance can be achieved by mounting the vehicle rotors in this particular fashion while implementing the appropriate actuation allocation algorithm.

The main result in this work concerns the actuator allocation problem, i.e., how the rotors should be placed in order to achieve fault tolerance, and it is independent of the adopted control technique. The detection of the failure has not been studied here, mainly because it strongly depends on the control technique, but will be addressed in the next step of our investigation.

Acknowledgment

This work has been sponsored through Agencia Nacional de Promoción Científica y Tecnológica, FONCYT PICT 2014-2055 (Argentina), Concurso de Iniciación a la Investigación ITBA 2016, Universidad Nacional de la Patagonia Austral (PI29/C066), and ITBA Grant ITBACyT-28.

References

[1] M. Saied, B. Lussier, I. Fantoni, C. Francis, H. Shraim, and G. Sanahuja, Fault diagnosis and fault-tolerant control strategy for rotor failure in an octorotor, in IEEE International Conference on Robotics and Automation, May 2015, pp. 5266-5271.

[2] D. Vey and J. Lunze, Structural Reconfigurability Analysis of Multirotor UAVs after Actuator Failures, in 54th Conference on Decision and Control, December 2015, pp. 5097-5104.

[3] D. Vey and J. Lunze, Experimental evaluation of an active fault-tolerant control scheme for multirotor UAVs, in 3rd International Conference on Control and Fault-Tolerant Systems, September 2016, pp. 119-126.

[4] G. P. Falcon, V. A. Marvakov and F. Holzapfel, "Fault tolerant control for a hexarotor system using Incremental Backstepping," 2016 IEEE Conference on Control Applications (CCA), Buenos Aires, 2016, pp. 237-242

[5] M. W. Mueller and R. D'Andrea, "Stability and control of a quadrocopter despite the complete loss of one, two, or three propellers," in IEEE International Conference on Robotics & Automation, Hong Kong, China, 2014, pp. 45-52.

[6] K.-Y. C. Guang-Xun Du, Quan Quan, "Controllability analysis and degraded control for a class of hexacopters subject to rotor failures," Journal of Intelligent Robotic Systems, 2014.

[7] T. Schneider, "Fault-tolerant multirotor systems," Master's thesis, Swiss Federal Institute of Technology (ETH), 2011.

[8] M. Achtelik, K.-M. Doth, D. Gurdan, and J. Stumpf, "Design of a multi rotor MAV with regard to efficiency, dynamics and redundancy," in AIAA Guidance, Navigation, and Control Conference, 2012.

[9] J. I. Giribet, R. Sánchez-Peña and A. Ghersin, "Analysis and design of a tilted rotor hexacopter for fault tolerance" IEEE - Trans. on Aerospace and Electronics Systems, 4, 52, 2016.

[10] C. Pose, J. Giribet and A. Ghersin "Hexacopter fault tolerant actuator allocation analysis for optimal thrust", Proceedings of International Conference on Unmanned Aerial Systems, 2017.

[11] P. Moreno, C. Pose, and J. I. Giribet, INS/ultrasound navigation system, in Congreso Argentino de Sistemas Embebidos, Actas del SASE, 2015.